

# Supporting information: Predicting stable lithium iron oxysulphides for battery cathodes

Bonan Zhu<sup>\*,†,‡</sup> and David O. Scanlon<sup>\*,†,¶,§,‡</sup>

<sup>†</sup>*Department of Chemistry, University College London, 20 Gordon St, Bloomsbury, London WC1H 0AJ, United Kingdom*

<sup>‡</sup>*The Faraday Institution, Quad One, Becquerel Avenue, Harwell Campus, Didcot, OX11 0RA, United Kingdom*

<sup>¶</sup>*Thomas Young Centre, University College London, Gower Street, London WC1E 6BT, United Kingdom*

<sup>§</sup>*Diamond Light Source Ltd., Diamond House, Harwell Science and Innovation Campus, Didcot, Oxfordshire OX11 0DE, UK*

E-mail: bonan.zhu@ucl.ac.uk; d.scanlon@ucl.ac.uk

## Formation energies from DFT calculations

Formation energies calculated using standard density functional theory are known to contain significant systemic errors. For example, those of many binary oxides are under-predicted due to the over-binding of molecular oxygen (using local/semi local functionals),<sup>1-3</sup> which can be corrected by applying a rigid energy shift. For transition metal (TM) oxides, additional errors arise from the localised d-electrons, and often the Hubbard correction is required. One way for obtaining the desirable  $U$  values is by fitting the formation energies<sup>4</sup> of TM oxides to those obtained experimentally. Still, energies of GGA+ $U$  calculations cannot be mixed with those from standard DFT. This can be overcome by applying another rigid energy shift

( $\Delta E_M$ ) to the GGA+U energies.<sup>5</sup> The two corrections mentioned above are used by the Materials Project<sup>6</sup> where the Hubbard correction is only applied to oxides and fluorides of transition metals, and standard GGA calculations are used for sulphides. A slightly different approach is used by the Open Quantum Materials Database,<sup>7</sup> where the GGA+U is used for all materials containing the transition metals, and the elemental energies are adjusted to obtain the best fit with the experimental formation energies.

In this work, we are mainly concerned about the stability of oxysulphides, where the competing phases are binary/ternary oxides and sulphides. We apply the Hubbard correction to the oxysulphides because Fe ions are expected to be in the +2 or +3 oxidation states, and it is also applied for sulphides. In contrast, the Materials Project’s approach computes the competing FeS and FeS<sub>2</sub> phases using standard GGA. To evaluate the schemes, the reaction energies of several reactions are computed and compared with the values obtained using experimental formation energies obtained from the Kubaschewski Table.<sup>81</sup> The differences between the theoretical and the experimental values are shown in Figure S1, where *All* refers to the scheme where GGA+U is used for all species, and *Oxide only* is calculated using GGA for sulphides, and with the  $\Delta E_M$  term applied to the oxides treated with GGA+U. The *MP-ORIG* refers to the data extracted directly from the Materials Project with their corrections applied. Note that the  $U_{eff}$  (4.0 eV) and  $\Delta E_M$  (1.787 eV) terms in *All* and *Oxide only* are refitted using the methodologies that *MP-ORIG* refers to,<sup>4,5</sup> and we are not able to reproduce the fitted values for the latter ( $U = 5.3$  eV,  $\Delta E_M = -2.733$  eV). Interestingly, our refitted  $U$  and the  $\Delta E_M$  terms are very close to the ones reported in the two methodology papers.<sup>4,5</sup> Recently, a revised correction scheme was proposed by the Materials Project group<sup>10</sup> and made available online. The results obtained using this scheme is labelled as *MP-2020* ( $U = 5.3$  eV,  $\Delta E_M = -2.256$  eV). We note the newer PBE\_54 PAW data set is used in this work with `Fe_pv` for Fe, `Li_sv` for Li, `O` for O and `S` for S. The Materials Project uses the same pseudopotential choices, but from an older set named PBE.

---

<sup>1</sup>Using the data from the NIST-JANAF<sup>9</sup> table gives very similar results.

The reaction  $\text{FeS} + \text{Li}_2\text{S} \longrightarrow \text{FeO} + \text{Li}_2\text{O}$  can be used as a benchmark for the treatment of sulphides. Since it does not contain any elemental phase, the errors involved with them have no effect. Assuming that most of the DFT errors come from the treatment of the Fe, having a formation energy that is too negative means that the oxides are overly favoured, and vice versa. As shown in Figure S1, using U for both oxides and sulphides makes FeO slightly favoured (the *All* scheme), whereas if it is only applied to the oxides, the FeS is more favoured (*Oxide only*). If one assumes that the  $\Delta E_M$  correction for mixing GGA/GGA+U is sufficient for oxides, this implies that the standard GGA calculation overly stabilise FeS. The same behaviour is found in oxides using plain GGA, where the errors from localised the d electrons are found to compensate some of that from the oxygen over-binding.<sup>4</sup> While applying U to only the oxides gives an error of similar magnitude here (*Oxide only*), we find that the inclusion of U is essential for the correctly predicting the relative stabilities of FeS polymorphs. Using standard PBE functional, the troilite phase ( $P\bar{6}2_c$ ), a rare mineral and whose experimental formation energy is available, is predicted to be more than 200 meV/per atom higher in energy compared to the tetragonal phase.<sup>11</sup> The data from Materials Project gives large negative errors for this particular reaction, the difference can be attributed to different calibrations and corrections. In fact, the data from the Materials Project appear to be incorrectly calibrated for reproducing the reaction energy of oxidizing FeO to Fe<sub>2</sub>O<sub>3</sub> and Fe<sub>3</sub>O<sub>4</sub> (shown in the *Fitting U for Fe* of Figure S1), nor does it reproduce the binary formation energies of iron oxides (shown in the *GGA+U/GGA Mixing* of Figure S1). The new material project correction (*MP-2020*) appears to be correctly calibrated to the binary oxide formation energies with a revised  $\Delta E_M$ , but it suffers from the same problem for the reaction energies of oxidising FeO, due to the inconsistent  $U_{Fe}$  calibration. On the other hand, both two sets of reaction energies are well reproduced by the **Oxide only** scheme, which is not a surprise, since it was to calibrated to reproduce them. The *All* scheme does not include the  $\Delta E_M$  term and hence is not expect to give accurate formation energies for iron oxides, but we are only interested in the competition between the quaternary and binary

phases here. Hence, the *All* scheme is most suitable for investigating the stabilities of the oxysulphides.

## Gibbs’s free energy at finite temperature using machined learned descriptors

The energies from the DFT calculations can only be used to access the thermodynamic stability at 0 K. At finite temperatures, the synthesisability of a material depends on its Gibbs’s free energy, but the incorporation of temperature effects is not trivial. The vibrational entropy may be accounted for using phonon density of states under the quasi-harmonic approximation, which can be very resource intensive. Recently, a machine learning model for estimating the Gibbs’s free energy has been reported.<sup>12</sup> In that work, it was found that the Gibbs energy may be estimated to a good accuracy using the 0 K enthalpy given by DFT plus an additional analytical term that is data mined using the sure independence screening and sparsifying operator (SISSO) method. This additional term only takes the composition of the material, the volume of the DFT relaxed structures, and the temperature as the input.

Applying this approach allows us to estimate the synthesisability at finite temperatures. In the Figure S2, the phases that are predicted to be close to the convex hull remain close at finite temperatures. Interestingly, the number of stable phases appears to increase with increasing temperature. This is reflected in both the computed distance to hull as well as the distance to hull formed by the known non-quaternary phases.

However, we note that these results under finite temperatures can have several caveats. First, the contribution of configurational entropy is not explicitly included, which could make disordered phases more favourable at high temperatures, and one example is the  $\text{Li}_2\text{FeSO}$ . Second, the physical descriptor was fitted using the Materials Project’s data, which are computed using a similar but not identical pseudopotential set. In addition, the U for Fe d electron is 4 eV here whereas the Materials Project uses 5.3 eV. This could result

in inconsistencies in the both the energies of Fe-containing phases and their equilibrium volumes. Second, the training and testing set of the descriptor only includes the known experimental phases, whereas here a large set of newly predicted structures also exists. Many metastable phases that have higher volume per atom are found by our search, giving much reduced  $G_{SISSO}^{\delta}$  term as a result of its volume dependency. In some cases, predicted phases that are more than 100 meV above the hull at 0K can be stabilised. Since such hypothetical structures are not included in the training set, result results are less reliable. As a result, we have to limit the phases considered in Figure S2 to those having the lowest DFT energy for each composition. Formation energies including free energy contributions under fixed volumes have been calculated using Phonopy, and compared with those predicted by SISSO as shown in Figure S3. Although a good agreement is found for  $\text{Li}_4\text{Fe}_3\text{S}_3\text{O}_2$ , those for  $\text{Li}_2\text{Fe}_2\text{S}_2\text{O}$  and  $\text{Li}_2\text{Fe}_3\text{S}_2\text{O}_2$  have rather large deviations. Since the SISSO descriptor is fitted with constant pressure data, phonon calculations using the quasi harmonic approximation may provided data that are more applicable for comparison. Such validation study would be beyond the scope of this work. Finally, it should be noted that the descriptor itself is found to have mean absolute error (MAE) of 46 meV as mentioned in the original paper,<sup>12</sup> although some degrees of the error cancellations are expected as only four elements are included.

## Data availability

The structure searching results, raw calculation data for phonon, NEB and hybrid functional calculations, an archive containing the provenance of all calculations for the AiiDA framework, and example notebooks for data analysis and plotting have been deposited into the Zenodo repository with open access. DOI: 10.5281/zenodo.4977231.

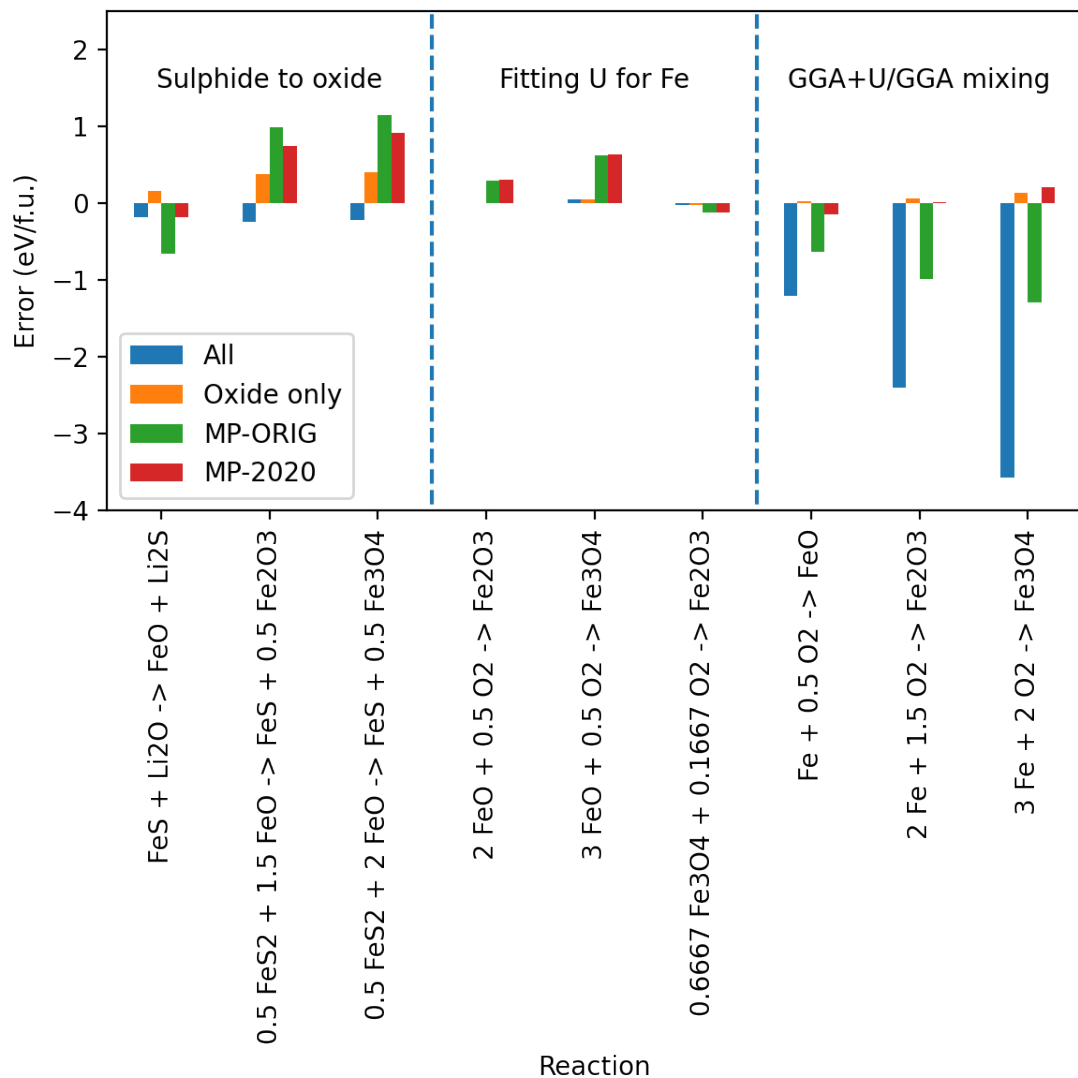


Fig. S1: Errors of the reaction energies using different schemes for treating Fe-containing oxides and sulphides with Hubbard correction. The *All* scheme uses  $U_{\text{Fe}} = 4.0\text{eV}$  for both oxide and sulphides. The *Oxide only* uses the  $U_{\text{Fe}} = 4.0\text{eV}$  for oxides but not for sulphides, and the GGA+U energies are corrected by a  $\Delta E_M$  term (1.787 eV) so it can be mixed with the GGA calculations. The *MP* scheme uses the same methodology as the *Oxide only*, but the energies are obtained directly through the Materials Project API using their settings and corrections ( $U_{\text{Fe}} = 5.3\text{eV}$ , and  $\Delta E_M = 2.733$ ).

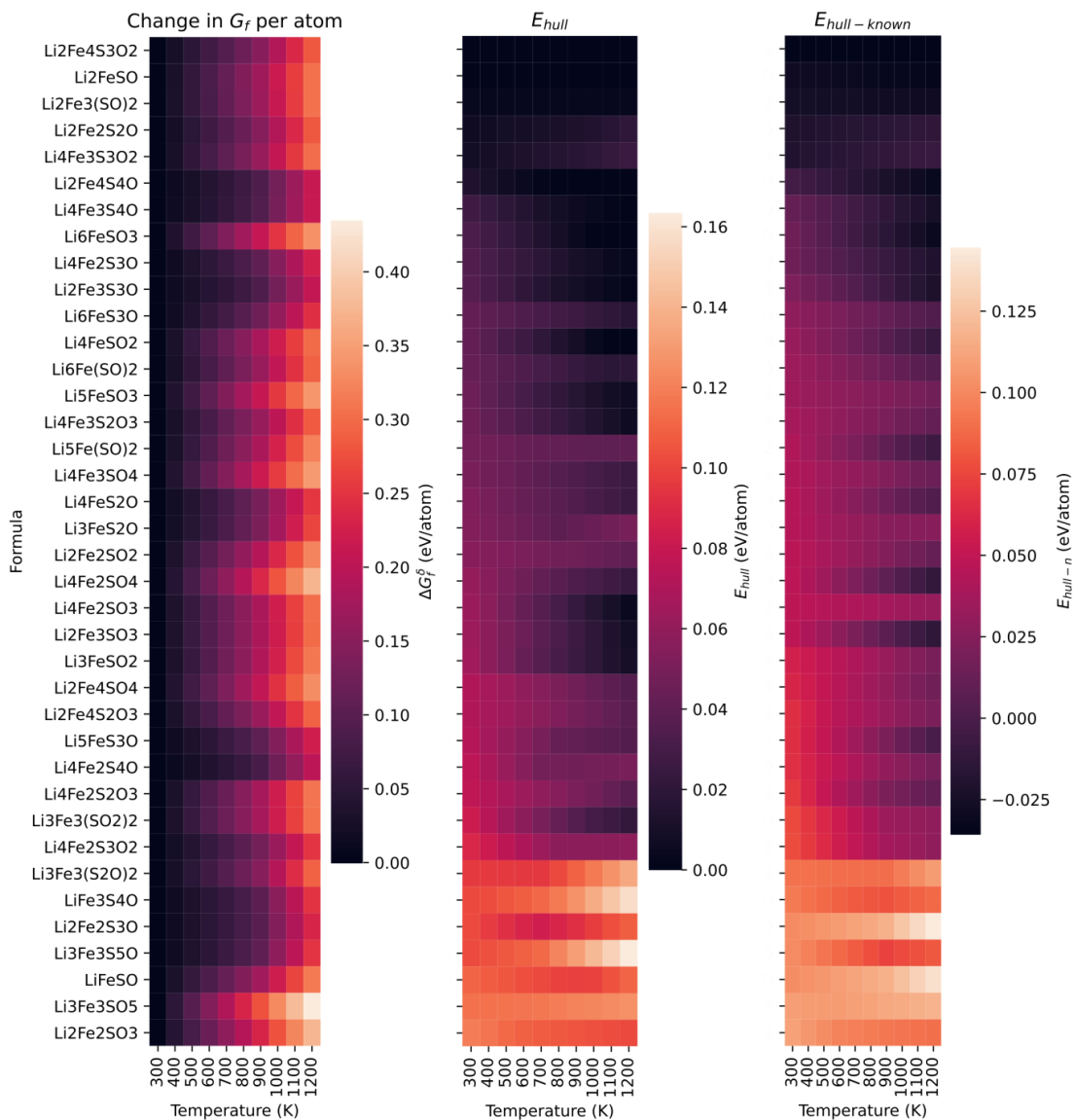


Fig. S2: Finite temperature stabilities predicted using the physical descriptors data mined by the SISSO method.<sup>12</sup> It can be seen that the stabilities of most phases does not change much with temperature, but there are exceptions.

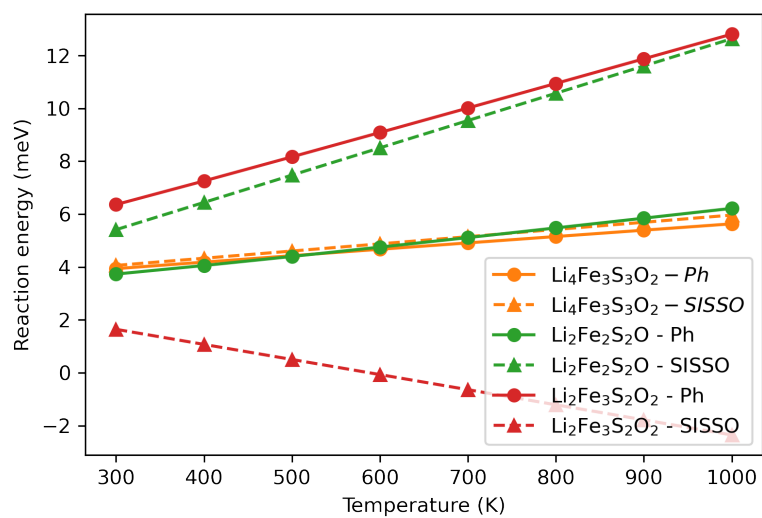


Fig. S3: Change in free energy calculated using phonopy compared to those estimated using the SISSO descriptor.

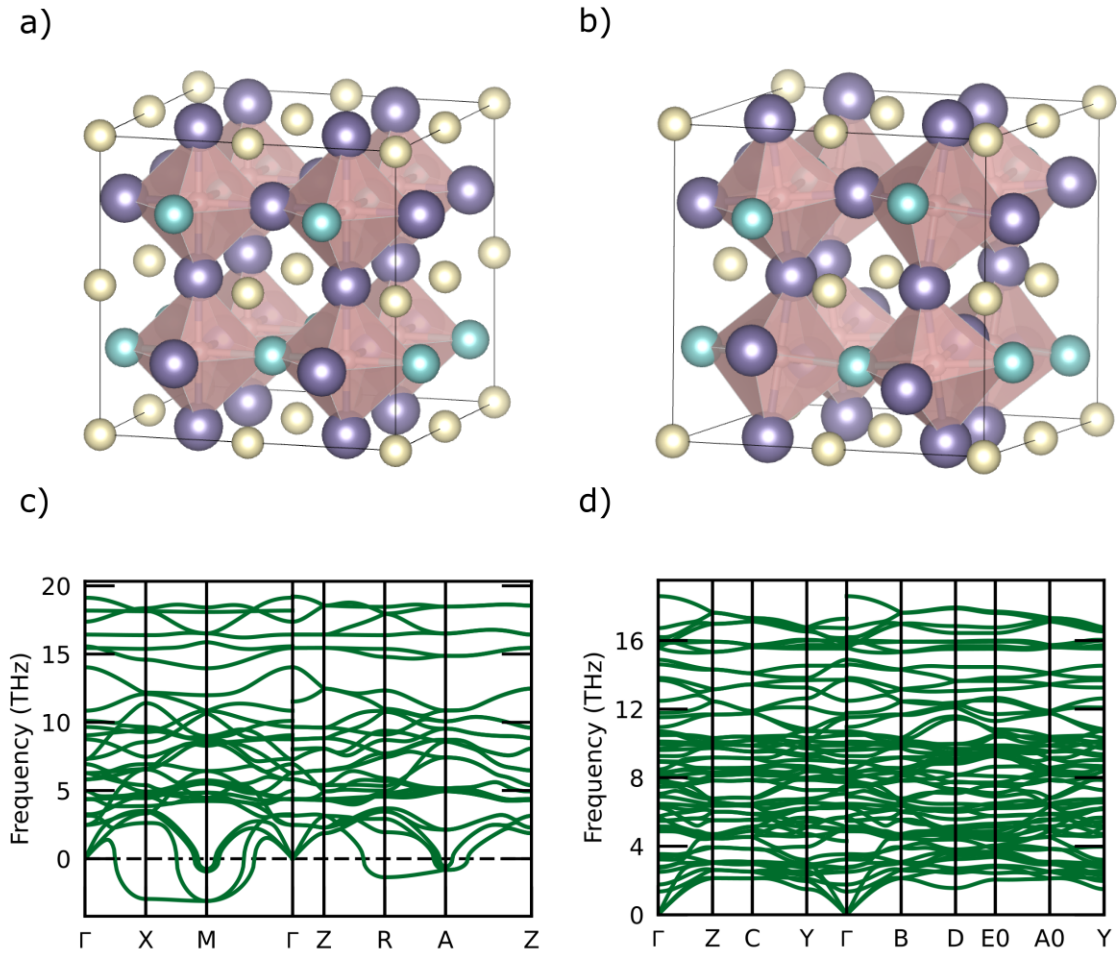


Fig. S4: (a) The ordered  $Li_2FeSO$  structure reported previously.<sup>13</sup> (b) The mode-pushed structure with  $a^-b^-c0$  tilted octahedra. (c) The phonon band structure of the order  $Li_2FeSO$  with imaginary frequencies. (d) The phonon band structure of the mode-pushed structure without any imaginary frequency. Colour coding: cream-S, purple-Li, cyan-Fe, pink-O.

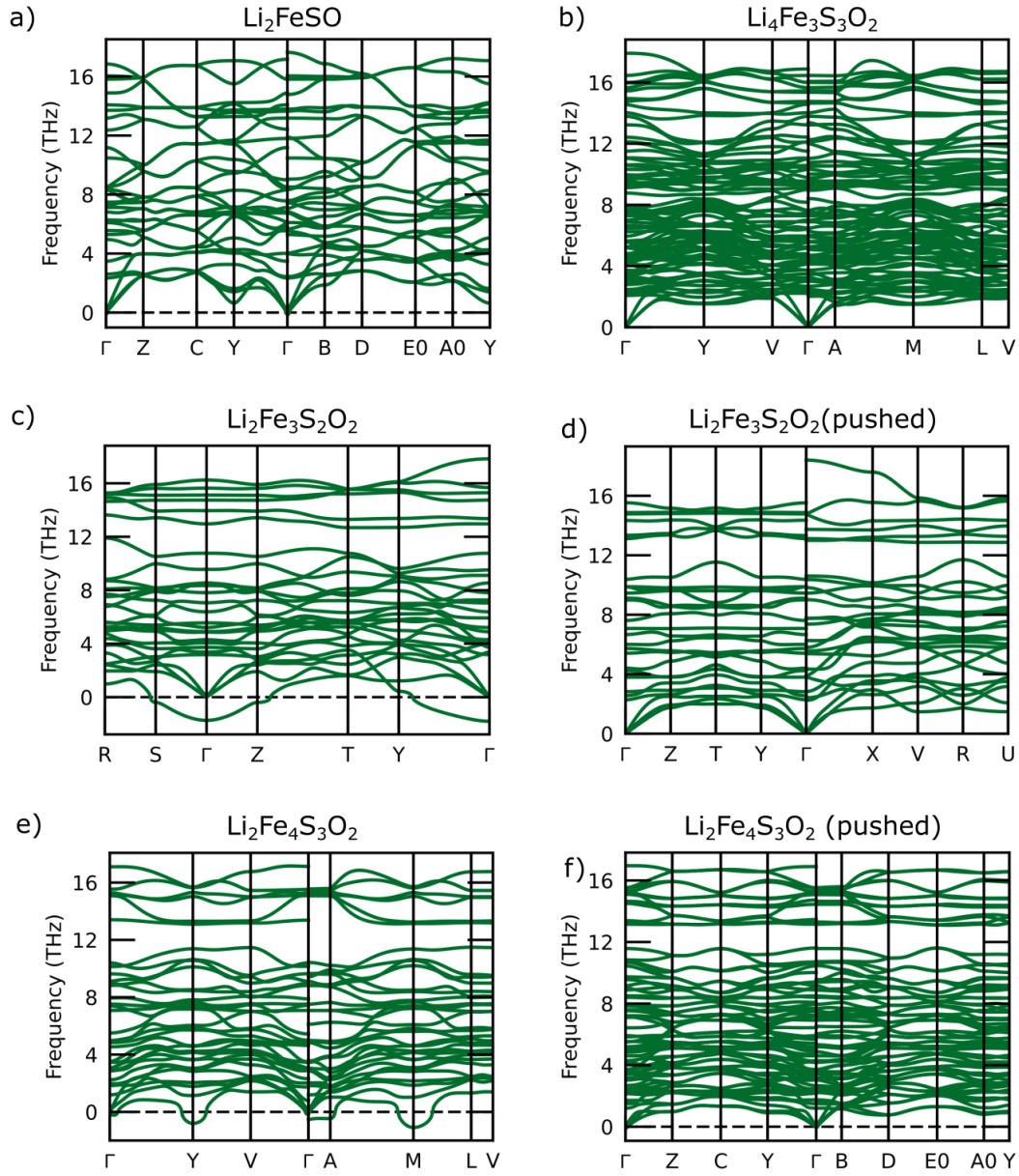


Fig. S5: Phonon dispersions calculated for (a)  $\text{Li}_2\text{FeSO}$ , (b)  $\text{Li}_4\text{Fe}_3\text{S}_3\text{O}_2$ , (c,d)  $\text{Li}_2\text{Fe}_3\text{S}_2\text{O}_2$  and (e,f)  $\text{Li}_2\text{Fe}_4\text{S}_3\text{O}_2$

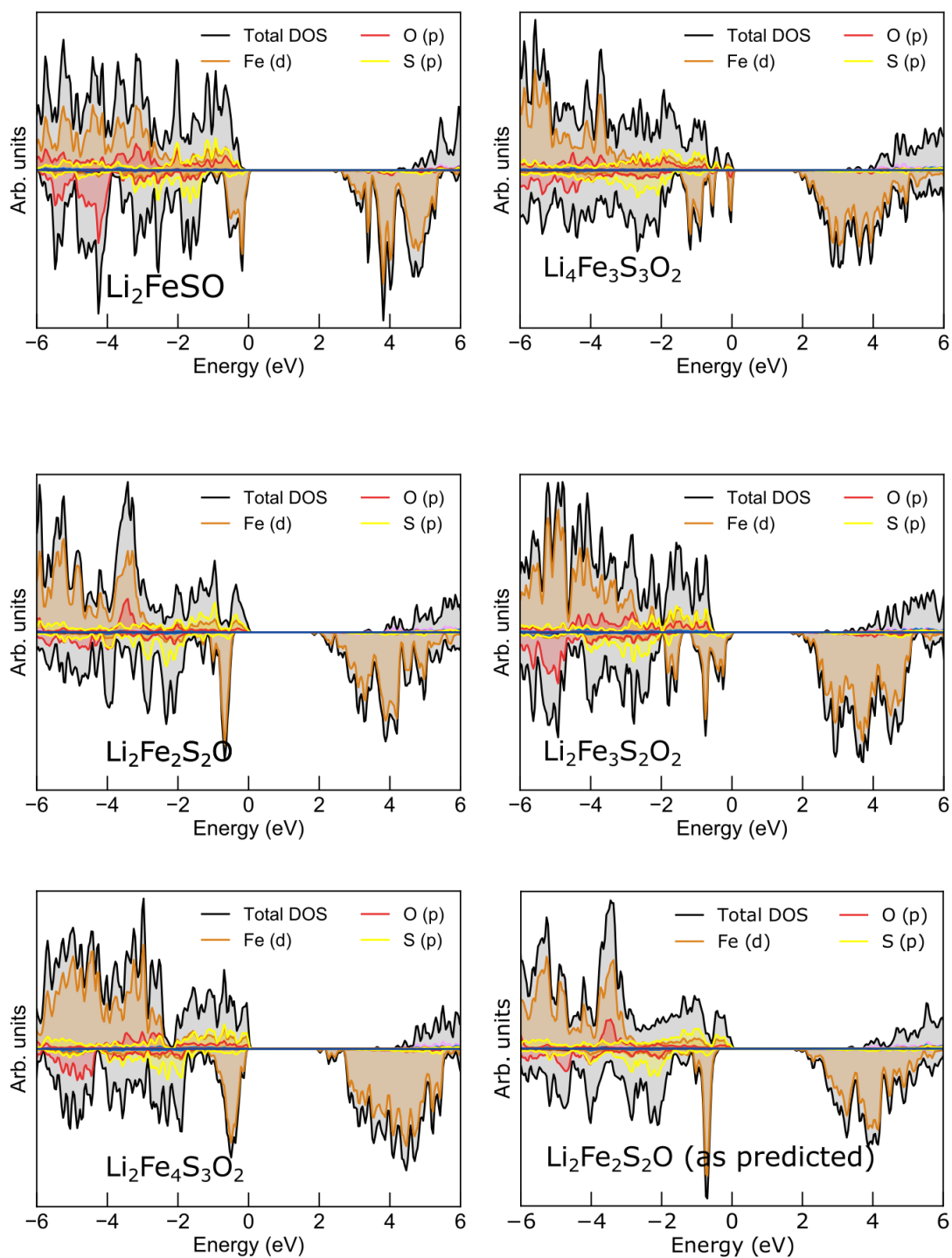


Fig. S6: Projected density of states for the predicted phases using HSE06 hybrid functional. The valence band tops are consisted of Fe d states, O p states and S p states, and the conduction band maximum is dominated by Fe d states. The band gaps of these materials are about 2 eV. Note that the mode pushed  $\text{Li}_2\text{Fe}_2\text{S}_2\text{O}$  and the as-predicted  $a\text{Li}_2\text{Fe}_2\text{S}_2\text{O}$  both have almost the same density of states<sup>S11</sup>

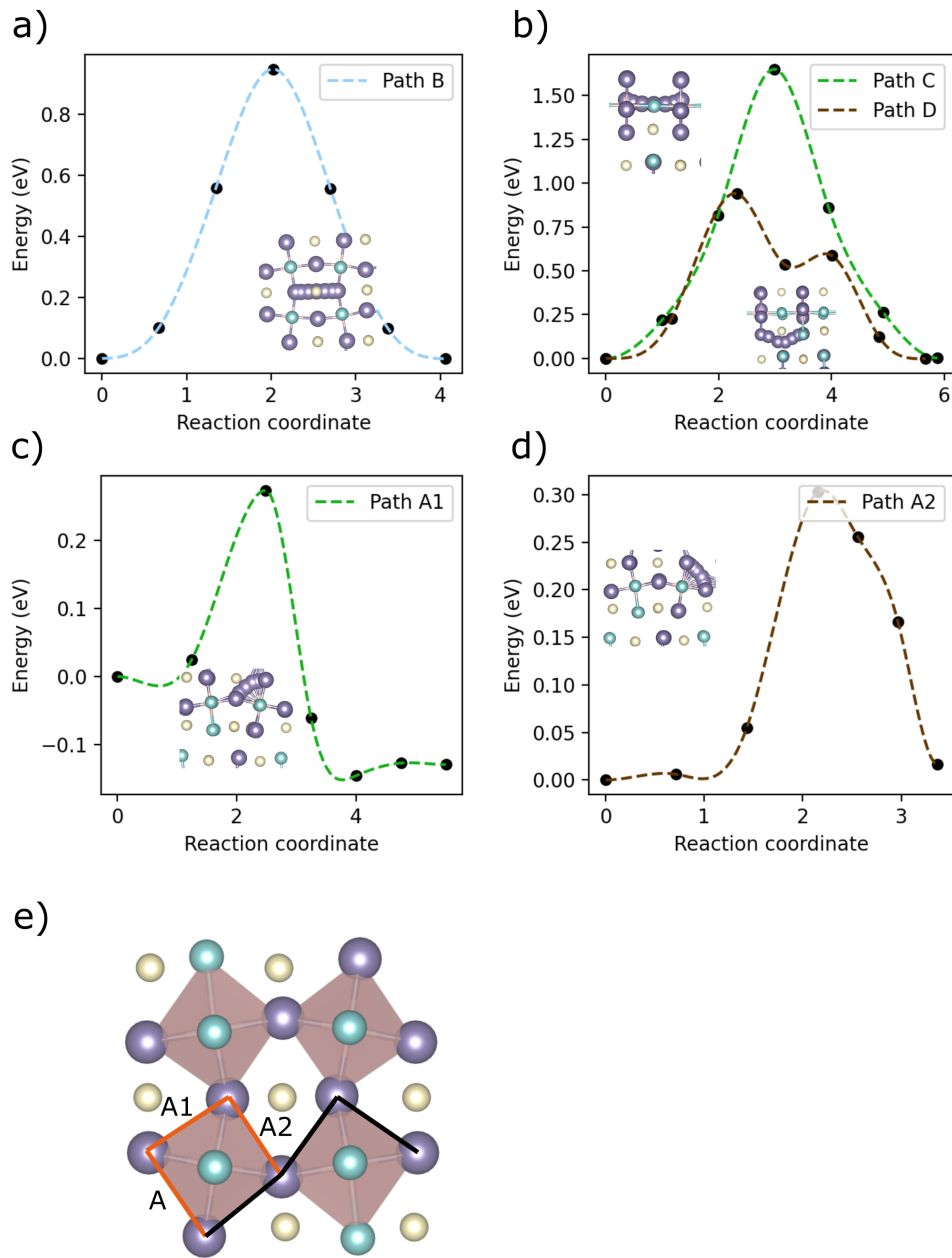


Fig. S7: Minimum energy transition pathways for next nearest neighbour hops for (a)  $\text{Li}_2\text{Fe}_2\text{S}_2\text{O}$  (showing only the perovskite layer) and (b)  $\text{Li}_4\text{Fe}_3\text{S}_3\text{O}_2$ . Additional NN pathways inside the perovskite layers for  $\text{Li}_4\text{Fe}_3\text{S}_3\text{O}_2$  are shown in (c) and (d). The six inequivalent NN pathways in the perovskite layers of  $\text{Li}_4\text{Fe}_3\text{S}_3\text{O}_2$  are shown in (e). Those with barrier heights calculated are coloured in orange. Colour coding: cream-S, purple-Li, cyan-Fe, pink-O.

## References

- (1) Jones, R. O.; Gunnarsson, O. The Density Functional Formalism, Its Applications and Prospects. *Reviews of Modern Physics* **1989**, *61*, 689–746.
- (2) Patton, D. C.; Porezag, D. V.; Pederson, M. R. Simplified Generalized-Gradient Approximation and Anharmonicity: Benchmark Calculations on Molecules. *Physical Review B* **1997**, *55*, 7454–7459.
- (3) Hammer, B.; Hansen, L. B.; Nørskov, J. K. Improved Adsorption Energetics within Density-Functional Theory Using Revised Perdew-Burke-Ernzerhof Functionals. *Physical Review B* **1999**, *59*, 7413–7421.
- (4) Wang, L.; Maxisch, T.; Ceder, G. Oxidation Energies of Transition Metal Oxides within the GGA+U Framework. *Physical Review B* **2006**, *73*, 195107.
- (5) Jain, A.; Hautier, G.; Ong, S. P.; Moore, C. J.; Fischer, C. C.; Persson, K. A.; Ceder, G. Formation Enthalpies by Mixing GGA and GGA + U Calculations. *Physical Review B* **2011**, *84*, 045115.
- (6) Jain, A.; Ong, S. P.; Hautier, G.; Chen, W.; Richards, W. D.; Dacek, S.; Cholia, S.; Gunter, D.; Skinner, D.; Ceder, G.; Persson, K. A. Commentary: The Materials Project: A Materials Genome Approach to Accelerating Materials Innovation. *APL Materials* **2013**, *1*, 011002.
- (7) Kirklin, S.; Saal, J. E.; Meredig, B.; Thompson, A.; Doak, J. W.; Aykol, M.; Rühl, S.; Wolverton, C. The Open Quantum Materials Database (OQMD): Assessing the Accuracy of DFT Formation Energies. *npj Computational Materials* **2015**, *1*, 1–15.
- (8) Kubaschewski, O.; Kubaschewski, O.; Alcock, C. B. *Metallurgical Thermochemistry*; Elsevier Science & Technology Books, 1979.

- (9) Allison, T. JANAF Thermochemical Tables, NIST Standard Reference Database 13. 1996.
- (10) Wang, A.; Kingsbury, R.; McDermott, M.; Horton, M.; Jain, A.; Ong, S. P.; Dwaraknath, S.; Persson, K. A Framework for Quantifying Uncertainty in DFT Energy Corrections. **2021**,
- (11) Lai, X.; Zhang, H.; Wang, Y.; Wang, X.; Zhang, X.; Lin, J.; Huang, F. Observation of Superconductivity in Tetragonal FeS. *Journal of the American Chemical Society* **2015**, *137*, 10148–10151.
- (12) Bartel, C. J.; Millican, S. L.; Deml, A. M.; Rumpitz, J. R.; Tumas, W.; Weimer, A. W.; Lany, S.; Stevanović, V.; Musgrave, C. B.; Holder, A. M. Physical Descriptor for the Gibbs Energy of Inorganic Crystalline Solids and Temperature-Dependent Materials Chemistry. *Nature Communications* **2018**, *9*, 4168.
- (13) Lu, Z.; Ciucci, F. Anti-Perovskite Cathodes for Lithium Batteries. *Journal of Materials Chemistry A* **2018**, *6*, 5185–5192.